

CHALLENGING PROBLEMS INVOLVING BENZENOID POLYCYCLICS AND RELATED SYSTEMS

Alexandru T. Balaban

The Polytechnic, Organic Chemistry Department, Bucharest, Roumania

Abstract - Five theoretical and/or experimental problems involving benzenoid polycyclics and related systems are discussed. The dualist graph characterizes uniquely any polycyclic aromatic hydrocarbon (PAH or polyhex), and differentiates between catafusenes, perifusenes and coronafusenes (catahexes, perihexes, coronahexes).

1. The topology of catafusenes, expressed by their dualist graphs, can be correlated with the rates of Diels-Alder addition to maleic anhydride (determined by Biermann and Schmidt, 1980). The most important topological parameter in this correlation is the number of rings in the longest acene portion of the catafusene. The topology at the ends of this longest acene portion constitutes the second parameter.
2. As known, the carcinogenic activity of PAH's is connected with the existence of bay-regions. Simple topological rules making use of dualist graphs can be implemented by means of a computer program to explore all PAH structures with or without bay-regions. However, the problem is much more complex, because there exist many PAH's with bay-regions that are not carcinogenic, and a few carcinogenic PAH's without a bay-region.
3. Owing to its remarkable structure of coronafusene, kekulene may afford aza-analogues which should lead to highly interesting metallic complexes. The number of possibilities is much higher than in the case of porphyrins and related structures. These possibilities are reviewed and their potential applications are highlighted. As yet, no experimental data are available, but such polydentate ligands represent an exciting synthetic challenge for organic chemists.
4. So far, no experimental determinations of "local ring current" or "benzene character" in PAH's exist, though the theory has been much discussed (Clar, Polansky, Herndon, Randić, Hosoya, Aihara, Gutman, Trinajstić, Bonchev). By means of proton NMR spectra of N-aryl-2,4,6-trimethylpyridinium salts (readily available from primary arylamines and 2,4,6-trimethylpyrylium salts), one can measure ring currents in the N-aryl group, and one should be able to calculate therefrom local ring currents. Experimental data with all isomeric naphthyl and anthryl groups show, however, that the theory of shielding is not precise enough: Johnson-Bovey's data yield too high, Haigh-Mallion's data too low effects relatively to the measured ones. Even using corrections for dihedral angles and C-N bond distances, discrepancies are too large.
5. By means of dualist graphs, a simple rule is devised for establishing whether a given polyhex is a free radical (mono- or poly-radical), or a normal compound possessing a Kekulé structure. However, there exists a class of diradicals which are not encompassed by this rule, so that a universal procedure for establishing simply whether a given PAH has, or does not have, Kekulé structures, has now been found (Appendix).

INTRODUCTION

Scope of this paper

In the lecture held at the International Symposium on Aromaticity (Dubrovnik, Croatia, Yugoslavia, 3-5 September 1979) under the title "Is Aromaticity Outmoded?" (Ref. 1), I tried to illustrate the idea that research on new and old aromatic systems is still an active area full of exciting and enticing unknowns, and at the end of that lecture I presented a few future prospects and general challenges. The present lecture is intended to be, in a certain respect, a continuation of the previous one, namely to discuss challenging, open research problems relating, however, only to a restricted area centered around condensed polycyclic benzenoid systems. Thus, rather than presenting one set of finished, complete results, it is hoped to convey better the

message that research involving aromatic structures is a living field, by bringing before you several pieces of still crudely shaped ideas and provisional results from our laboratory, hoping also that some of these ideas may benefit from discussions or collaborations, or may serve as incentive for other research groups.

Polyhexes and their dualist graphs

Polycyclic benzenoid hydrocarbons (or polyhexes, or Polycyclic Aromatic Hydrocarbons, to be abridged as PAH's) are structures composed only of condensed benzenoid rings, wherein all carbon atoms have sp^2 - hybridization. Their hydrogen-depleted graphs are portions of the graphite (honeycomb) lattice. Unless otherwise stated, the following discussion will only deal with systems devoid of side-chains.

Balaban and Harary (Ref. 2) proposed to characterize all PAH's by their dualist (characteristic) graphs, consisting of vertices situated at the centres of benzenoid rings, and of edges connecting vertices corresponding to condensed benzenoid rings. Such graphs are related to the dual graphs which are well known in Graph Theory, but differ from them because in dualist graphs (i) no vertex exists corresponding to the outer region, therefore dualist graphs are related to internal duals, and (ii) angles are important, unlike any other graphs.

These dualist graphs have become an accepted tool for characterizing the topology of polyhexes, for nomenclature and coding purposes (Refs. 3 and 4), and for the classification of polyhexes (PAH's) into three classes :

(1) catafusenes (catahexes), when the dualist graphs are trees (i.e., have no cycles) ;

(2) perifusenes (perihexes), when the dualist graphs have three-membered rings (possibly in addition to tree-like branches as side-chains) ;

(3) coronafusenes (coronahexes), when the dualist graphs have larger rings (8-, 10-, or larger-membered rings, possibly in addition to three-membered rings and side-chains. A special group of coronafusenes is represented by corannulenes which were discussed by Agranat, Hess and Schaad (Ref. 5) : the dualist graphs of corannulenes is a single ring of 8 or more vertices. More will be said about corannulenes in a later Section of this paper.

On the basis of these ideas, an enumeration of non-branched (Ref. 2) and branched catafusenes (Ref. 6) was possible. Polansky and Rouvray have formalized the description of polyhexes by means of dualist graphs (Refs. 7 and 8).

The three-digit code developed for catafusenes (Refs. 2 and 3) symbolizes linear annelation by digit 0, and kinked annelation by digits 1 or 2 for clockwise or anticlockwise kinks, respectively, in following the dualist graph from one endpoint of the graph, with the proviso that the code should correspond to the lowest possible number formed from these digits when there are several alternatives. This is illustrated by Fig. 1.

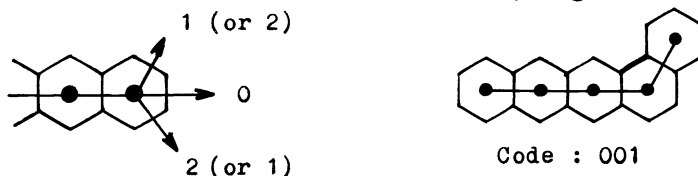


Fig. 1. Exemplification of three-digit code for catafusenes.

A correspondence exists between the three-digit code of catafusenes and the coding system for staggered alkane rotamers (Refs. 9 and 10) which can act as dualist graphs for three-dimensional portions of the diamond lattice, i. e., for diamond hydrocarbons like triamantane, tetramantane, etc. A coding and nomenclature system was accordingly devised for such diamond hydrocarbons by Balaban and Schleyer (ref. 10).

Ref. 11 shows that resonance energies of catafusenes are linearly dependent on the number of zero digits in their three-digit code, and in the number of benzenoid rings. Most properties do not differ if digits 1 and 2 are interchanged (an example will be given in the next Section), so that the three-digit code may be converted for certain purposes into a topological index for catafusenes by the "L-transform of their three-digit codes", wherein digits 1 and 2 are replaced by 1 and the resulting code is read as a binary number for non-branched catafusenes (Ref. 12). This topological index can serve the same purposes

as the sextet polynomial introduced by Hosoya and Yamaguchi (Ref. 13). However, for branched catafusenes the L-transform needs additional conventions, and it is not applicable to perifusenes.

TOPOLOGICAL CORRELATIONS BETWEEN STRUCTURE AND REACTION RATE FOR PAH'S

Usually for quantitative structure-activity relationships the chemical structure is analyzed in terms of electronic, steric or hydrophobic interactions. A new trend which has developed rapidly in the last two decades converts the chemical structure into topological indices (Ref. 14). In the present Section we shall develop a mathematical model for a topological correlation between the chemical structure of catafusenes and their reaction rate with maleic anhydride in Diels-Alder cycloadditions. Biermann and Schmidt (ref. 15) have determined with a sensitive spectrophotometric technique and with high precision these second-order reaction rates k_2 for a large range of 46 catafusenes. These reaction rates span a range of relative values from 1 to 5,000,000 and are therefore conveniently expressed in logarithmic form, $6 + \lg k_2$.

For rationalizing the observed rate constants, Biermann and Schmidt carried out MO calculations (Ref. 15), determining para-localization energies P after Brown, and second-order stabilization energies $\Sigma E^{(2)}$ using a semi-empirical perturbational approach based on HMO-calculated ionization potentials (instead of Fukui's treatment which proved unsatisfactory). For a more restricted group of 21 catafusenes whose first two ionization potentials IP_1 and IP_2 were known from photoelectron spectra, they also obtained satisfactory correlations with the difference $\Delta IP = IP_2 - IP_1$, or a weighted difference between these ionization potentials. These last correlations suggest that UV data should also correlate with the Diels-Alder reactivity, as was noticed earlier by Clar; indeed, a weighted difference between the experimentally determined energies E_β and E_p of the β - and p -bands in the electronic absorption spectrum correlates well with the observed reaction rates. All these correlations and the resulted standard deviations are summarized in Table 1.

TABLE 1. Correlations between reaction rates of catafusenes expressed as $(6 + \lg k_2)$ and quantum-chemical parameters after Biermann and Schmidt (ref. 15)

$6 + \lg k_2 =$	Standard deviation	Number of catafusenes
$= 49.10 + 13.59 P$	0.410	
$= -46.84 - 334.74 \Sigma E^{(2)}$	0.283	
$= 0.029 + 3.983 (IP_2 - IP_1)$	0.589	21
$= 17.28 + 7.52 (0.347 IP_2 - 0.653 IP_1)$	0.265	
$= 9.107 + 5.758 (0.283 E_\beta - 0.717 E_p)$	0.287	
$= 48.53 + 13.49 P$	0.361	46
$= -46.08 - 328.32 \Sigma E^{(2)}$	0.274	

It has been known for a long time that the results of the Hückel MO theory are solely and entirely determined by the carbon-atom connectivity (the topology) of the conjugated system under investigation (Refs. 16-19). Therefore one could expect the existence of short-cuts connecting more directly the molecular topology with the experimental data (which in our case are the reaction rates), obviating the need for elaborate MO calculations. As expression of the molecular topology we use the dualist graph, and we note from Biermann and Schmidt's original papers that no diene reactivity towards maleic anhydride is observed unless the catafusene possesses at least three linearly condensed benzenoid rings, i. e. an anthracene moiety. We therefore use as the main topological parameter the number n of edges in the longest rectilinear portion of the dualist graph, representing thus the longest acene portion of the catafusene: for anthracene $n = 2$, and for pentacene $n = 4$.

On representing the reaction rates $(6 + \lg k_2)$ versus $\lg n$ (Fig. 2), it is apparent that the reaction rates of all 46 catafusenes follow a general trend which can lead to a simple mathematical model: depending on the geometry at the ends of the longest rectilinear portion of the dualist graph, all 46

points fall on a converging family of straight lines, having a common point ($n = 14, 6 + \lg k_2 = 10.6$). The nine straight lines which fan out at regular angles from this point are determined by the topological rules presented in Table 2. Equations of these straight lines and calculated reaction rates are presented in Tables 3 and 4. The standard deviation for all 46 points is 0.114 which is much less than the values from Table 1. As seen from Table 4 for compounds No. 4, 24 and 43, there are only three deviations as large as 0.21-0.31, most of the deviations being lower than 0.1.

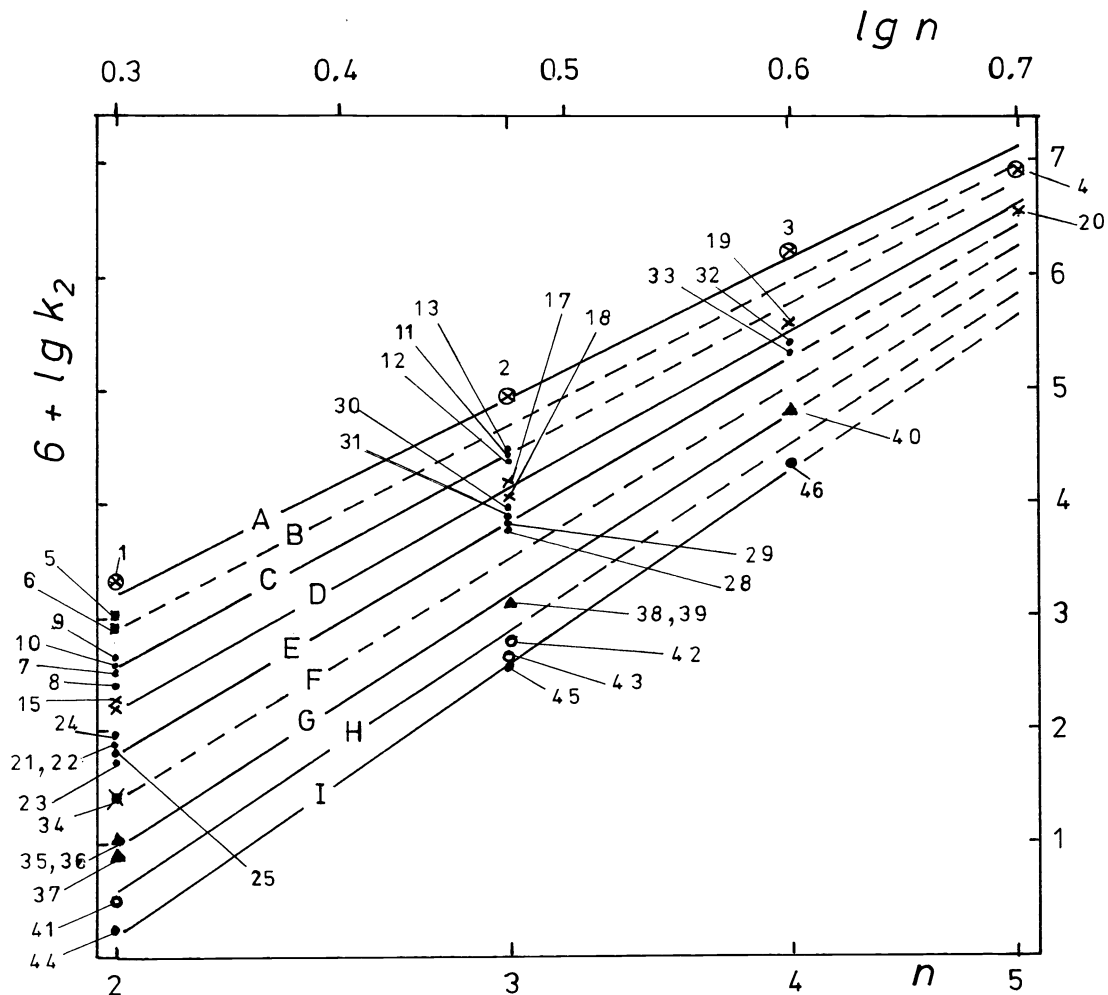


Fig. 2. Plot of Diels-Alder reaction rates of catafusenes with maleic anhydride (numbering of catafusenes as in Table 4) versus $\lg n$. The nine straight lines are denoted A-I according to Tables 2-4.

Some comments on the topological rules presented in Table 2 are necessary. Since only the largest acene portion is relevant, smaller acene portions act only by influencing the geometry at the end(s) of the largest acene portion. When the molecule possesses several equally longest acene portions, only that portion is "active" which has the less substituted end(s) according to Rules 1 and 3 from Table 2, because only the more reactive portion determines the reaction rate. The column labelled "effect" indicates the number of upward (+), or downward (-), jumps between successive lines A-I on effecting each type of annelation (the newly added ring is symbolized by a white point of the dualist graph). When a line may be reached from above or from below, the result is discriminated by prime symbols (' or ") following the indication of the line in Tables 2 and 4, but not in Fig. 2 or in Table 3.

Outstanding features in this correlation are :

(1) The large positive effect of collinear annelation of an acene (increasing

TABLE 2. Topological rules for the assignment of catafusenes to one of the straight lines in Fig. 2.

Rule	A n n e l a t i o n	Effect	E x a m p l e
1		- 3	A → D ; D → G
2		+ 1	D → C ; G → F ; E → D'
3		- 1	D → E ; G → H ; H → I
4		+ 1	E → D'' ; C → B
5		- 1	D → E'
6		0	E → E''

TABLE 3. Equations of straight lines A-I and rate constants ($6 + \lg k_2$) calculated therefrom ; in brackets, predicted values without experimental counterparts ; values without brackets are compared with experimental ones in Table 4.

Type	Line	E q u a t i o n	n = 2	n = 3	n = 4	n = 5
	A	$9.74 \lg n + 0.28$	3.21	4.93	6.14	7.09
	B	$10.14 \lg n - 0.15$	2.90	(4.69)	(5.95)	(6.94)
	C	$10.58 \lg n - 0.61$	2.57	4.44	(5.76)	(6.79)
	D	$11.16 \lg n - 1.23$	2.13	4.09	5.49	6.57
	E	$11.66 \lg n - 1.76$	1.79	3.80	5.26	(6.39)
	F	$12.16 \lg n - 2.29$	1.37	(3.51)	(5.03)	(6.21)
	G	$12.68 \lg n - 2.84$	0.98	3.21	4.79	(6.02)
	H	$13.21 \lg n - 3.40$	0.58	2.90	(4.55)	(5.83)
	I	$13.75 \lg n - 3.98$	0.16	2.58	4.30	(5.63)

TABLE 4. Structures of catafusenes (expressed through their dualist graphs), and Diels-Alder reaction rates (experimental data after Biermann and Schmidt, calculated data after Table 3). Straight line designations A-I after Fig. 2 and Tables 2 and 3.

C a t a f u s e n e Number	Dualist graph	n	Line	Reaction rate ($6 + \lg k_2$)	
				Experim.	Calculated
1		2	A	3.36	3.21
2		3	A	4.97	4.93
3		4	A	6.22	6.14
4		5	A	6.82	7.09

5		2	B	3.03	2.90
6		2	B	2.93	2.90

TABLE 4 (continued)

C a t a f u s e n e				Reaction rate ($6+\lg k_2$)	
Number	Dualist graph	n	Line	Experim.	Calculated
7		2	C	2.58	2.57
8		2	C	2.44	2.57
9		2	C	2.68	2.57
10		2	C	2.62	2.57
11		3	C	4.41	4.44
12		3	C	4.39	4.44
13		3	C	4.43	4.44
14		2	D	2.13	2.13
15		2	D''	2.20	2.13
16		2	D'	2.15	2.13
17		3	D	4.23	4.09
18		3	D'	3.93	4.09
19		4	D	5.65	5.49
20		5	D	6.48	6.57
21		2	E	1.83	1.79
22		2	E'	1.82	1.79
23		2	E'	1.74	1.79
24		2	E'	2.00	1.79
25		2	E''	1.78	1.79
26		2	E''	1.77	1.79
27		2	E''	1.82	1.79
28		3	E	3.77	3.80
29		3	E'	3.82	3.80
30		3	E'	3.97	3.80
31		3	E''	3.90	3.80
32		4	E	5.45	5.26
33		4	E'	5.37	5.26

TABLE 4 (continued)

Number	Dualist graph	n	Line	Reaction rate ($6+\lg k_2$)	
				Experim.	Calculated
34		2	F	1.45	1.37
35		2	G	1.02	0.98
36		2	G	1.02	0.98
37		2	G	0.91	0.98
38		3	G	3.08	3.21
39		3	G	3.09	3.21
40		4	G	4.88	4.79
41		2	H	0.53	0.58
42		3	H	2.76	2.90
43		3	H	2.59	2.90
44		2	I	0.24	0.16
45		3	I	2.38	2.58
46		4	I	4.34	4.30

by 1 the value of n) : the additional rate increase tends, however, to become logarithmically smaller as n increases.

(2) The marked negative effect of "kinked annelation" of an acene (Rule 1) at either end of the longest acene portion.

(3) The small negative effect (Rule 3) of "branching annelation" when the newly added ring becomes attached to a bay-region (which will be defined in the Section on carcinogenicity) ; the similar effect of a collinear annelation after a bay region (Rule 5), and the null effect of a branching annelation when there is no bay-region (Rule 6) are to be contrasted to Rule 4 which indicates a small positive effect if the longest acene portion is parallel to the collinear annelation after a bay-region.

(4) Interestingly, Rule 2 shows a small positive effect of a kinked annelation after a bay-region. The direction of the kink (coded by digits 1 or 2 in the three-digit code) is irrelevant, as illustrated by comparing the reaction rates of compounds 35 or 36, and 38 or 39. In this respect, one may recall that the "L-transform" of the three-digit code ignores the difference between the digits 1 and 2, and only indicates if the annelation is collinear or kinked (Ref. 12) : the information thus provided is essentially similar to that conveyed by Hosoya's sextet polynomial (Ref. 13). Apparently, this kind of information is important for rates of the Diels-Alder reaction, so that one may hope that this information will eventually be available for all catahexes as a topological index. Thus instead of a two-parametric correlation such as the present one, a monoparametric correlation ought to be possible.

Still, this crude mathematical model (which, like any such model does not try to afford any explanation of the underlying phenomenon), using as main parameter the value of n and as additional criterion the assignment to one of the straight lines A-I according to the topological rules from Table 2, is able to rationalize and predict a large amount of data without any elaborate calculations, namely all rate constants with and without brackets from Table 3. It is also fairly certain that the rate of the dibenzopentacene related to compound 40 (Table 4) as the dibenzotetracene 38 is related to 39, or as 36 is related to 35, will have a very similar reaction rate to that exhibited by compound 40.

It is an open problem to try and explain why this model works, and why the straight lines from Fig. 2 meet at a common point around $n = 14$.

TOPOLOGY OF BAY-REGIONS AND CARCINOGENICITY OF POLYHEXES (PAH's)

The cancer scare needs hardly any emphasis. Not only has cancer nowadays become the second major cause of death in developed countries by suppression or elimination of infectious diseases, but it has increased in absolute numbers of cases. Apparently the polluted environment contributes substantially to this increased risk factor. Polycyclic aromatic hydrocarbons and nitrosamines are present in tobacco smoke, in exhaust gases, in smoked aliments, etc. An estimated rate of 1.3 billion grams per year of benzo[a]pyrene which is a potent carcinogen in milligram amounts, is released into the environment in the USA alone (Refs. 20, 21).

After the initial proposals by French theoretical chemists (Refs. 22, 23) that certain regions (K and L with particular electronic features) in PAH's are responsible for the carcinogenic activity, it was demonstrated by Jerina and his co-workers from the N.I.H. (Bethesda, Maryland) that diol-epoxides at a benzenoid ring belonging to a bay-region are the ultimate carcinogens (Refs. 24-26). Virtually any PAH having a bay-region also incorporates a K-region, so that the Pullmans and Daudels had guessed right.

A bay-region is defined as one benzenoid ring condensed angularly to a PAH skeleton (in Fig. 3, the broken lines may be C-C or C-H bonds, but the benzenoid ring adjacent to the bay-region must have four C-H bonds since here the diol-epoxide will be formed). By nucleophilic attack on the epoxydiol, DNA becomes irreversibly bonded to PAH residues. The ring-opening of the epoxide ring as indicated by the curved arrow is facilitated by the presence of the adjacent bay-region.

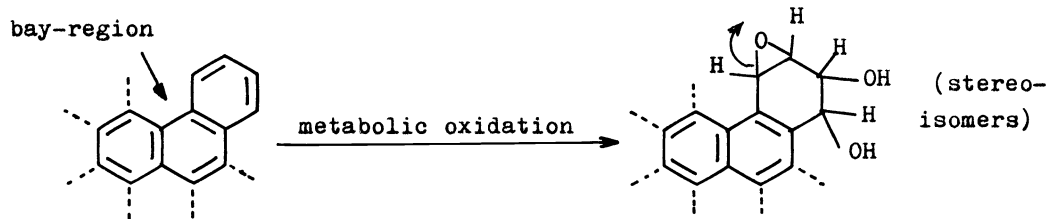


Fig. 3. Bay-region of a PAH and formation of a diol-epoxide.

Since it admits a simple topological definition, a bay-region may be alternatively defined by means of the dualist graph: a bay-region is present in a PAH if its dualist graph has an endpoint adjacent to a kink, i. e. if the edge starting from the endpoint forms with an adjacent edge an angle of 120° . In the following formulas, only the first three carcinogenic PAH's have bay regions because they have a kink adjacent to one endpoint of the dualist graph; the fourth non-carcinogenic pentaphene has a kink which is not adjacent to an endpoint, while the fifth non-carcinogenic perylene has no endpoint.

Polyhexes with bay-regions ;

and without bay-regions

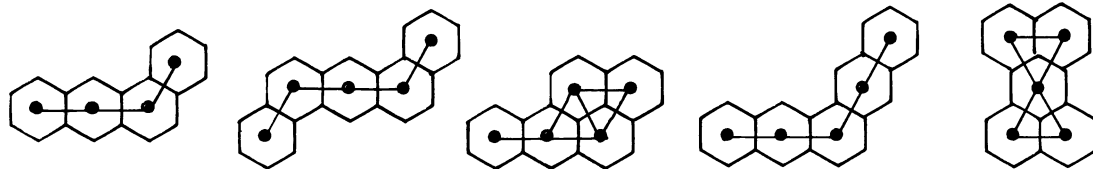


Fig. 4. Three PAH's with bay-regions and two without bay-regions.

Together with Dr. K. Balasubramanian and Professors Joyce J. Kaufman and W. S. Koski from the Johns Hopkins University, a computer program was elaborated and published for generating PAH's and identifying bay-regions (Ref. 27). The program generates non-branched and branched catafusenes (it also accomodates perifusenes) and prints out the three-digit code and the number of bays for each structure. It also prints or displays the structural formula of the PAH. For catafusenes, bays are counted by a scan algorithm which starts from one endpoint of the dualist graph (which is not always that one ending up in the minimal number, the actual code). The existence of a bay-region at the i -th stage depends on the i -th digit of the code (which must be 1 or 2 symbolizing a kink) and on the degree of the i -th vertex or of vertices two edges away from the i -th vertex (which degree must be 1 to symbolize one endpoint of the dualist graph). A counter keeps track of the bays at each stage i , and it prints out the number of bays at the end of the scan.

Useful as it is, this program cannot overcome the handicaps of this difficult research field :

(1) The presence of one or more bay-regions is not sufficient for carcinogenicity. Indeed, for many PAH's with bay-regions which were tested, no carcinogenic activity was found (Ref. 28).

(2) Though most of the proven carcinogenic PAH's do have bay-region(s), a few PAH's devoid of bay-regions still induce cancer, presumably by a different metabolic mechanism. Two examples are the moderate carcinogens presented in Fig. 5 (Ref. 28).

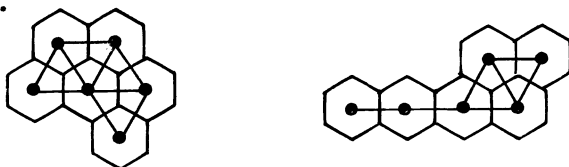


Fig. 5. Two moderate carcinogenic PAH's having no bay-region.

(3) Progress in theoretical research is hampered by the difficulty facing quantitative structure-activity relationships (QSAR) in this area of carcinogenic activity. The difficulty consists less in converting the structure of PAH into parameters which may be used in correlations, but more in the carcinogenic activity data. The older data like the Iball index (Refs. 29, 30) :

$$\text{I.C.I.} = 100 \frac{\% \text{ tumors}}{\text{days of latent period}}$$

have the advantage that they are numerical parameters with a continuous variation leading to facile correlations (Ref. 31), but in 1935-1940 when they were obtained the lots of animals were small and the genetic strains uncertain. Today's data, on the other hand (Ref. 28), are free from the above drawbacks, but are presented in discrete, discontinuous steps (e. g., inactive, disputed, moderately, and highly active), and this puts severe limitations on QSAR, leading to very approximate correlations (ref. 32).

Obviously, this is a serious and highly rewarding challenge which could profit enormously from international co-operation, possibly also involving WHO and UNESCO support : the PAH's are the oldest documented chemical carcinogens, their mode of action has recently become better understood, they probably represent one of the most aggressive noxious agents in the present-day environment, and yet their quantitative carcinogenic activity is so poorly defined and reported in the literature as to make meaningful QSAR almost impossible.

METALLIC COMPLEXES OF POLY-AZA-KEKULENES

The brilliant synthesis of the first authenticated coronafusene, kekulene, by Staab and co-workers (Ref. 33) opens a new vista in the study of PAH's. These authors established from proton NMR spectra that the structure ought to be represented by the first rather than the second formula in Fig. 6, because there is no abnormal shielding of inner protons, as it would result if the latter formula were the correct structure, with two concentric annulene rings bridged by single bonds. The bond lengths also indicate that the former formula is the correct representation for kekulene (Refs. 33, 34), and suggests that the third formula, patterned after Clar's ideas, is also a suitable representation. Since the dualist graph of kekulene is a single ring of 12 vertices, this PAH belongs to the special class of coronafusenes termed corannulenes (Ref. 5). Though discussed for a long time (Refs. 5, 8, 35, 36),

coronafusenes have posed a difficult synthetic problem. A corannulene with ten benzenoid rings was claimed to have been prepared in 1965 (ref. 37), but this claim is disputed (Refs. 33, 34).

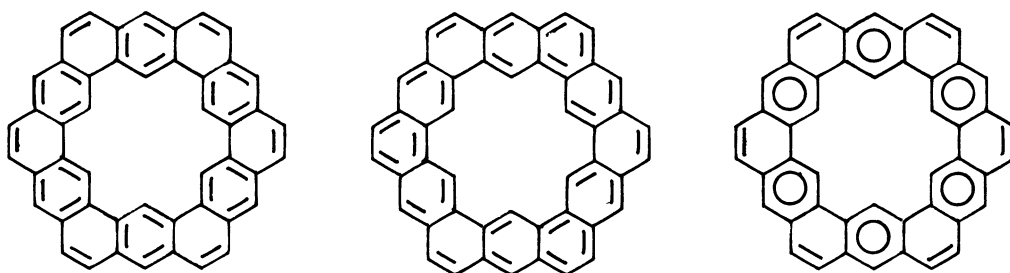


Fig. 6. Kekulene formulas (only the first and last ones are correct).

The kekulene framework offers considerable promise for exciting chemistry of metallic complexes having as chelating ligand a kekulene molecule in which all or part of the inner CH groups are replaced by nitrogen heteroatoms. We will only concentrate on the tri-, tetra-, penta-, and hexa-aza-kekulenes.

From the three possible isomeric triaza-kekulenes, the most interesting is the symmetrical one leading to trigonal coordination in the equatorial plane. The metals suitable for such coordination are those prone to forming trigonal-bipyramidal complexes, e. g. bismuth, leaving two free apical positions for other ligands, similarly to the coordination of iron with porphyrin ligands.

More interesting is the rectangular coordination offered by one of the three possible tetra-aza-kekulenes. Owing to the larger "hole" of polyazakekulenes than of porphyrins, not only iron, but also heavier transition metals from the eighth and other groups of the Periodic Table ought to coordinate. It will be interesting to test the difference between square coordination as with porphyrins, and the less symmetrical tetragonal coordination of the three tetra-aza-kekulenes.

Penta-aza-kekulene ought to lead to a distorted pentagonal-bipyramidal coordination with heavy transition metals.

Finally, hexa-aza-kekulene is expected to lead to very interesting metallic complexes with heavy transition metals having d- or f-orbitals, and presenting octa- or higher coordination. The interest of all these complexes (Fig. 7) is derived from the fact that the polyaza-kekulene ligands, like porphyrins (and unlike crown ethers or other criptands which are flexible non-planar ligands) are rigid planar or quasi-planar ligands which enforce a certain hybridization on the chelated metal atom, leading to fascinating chemical consequences.

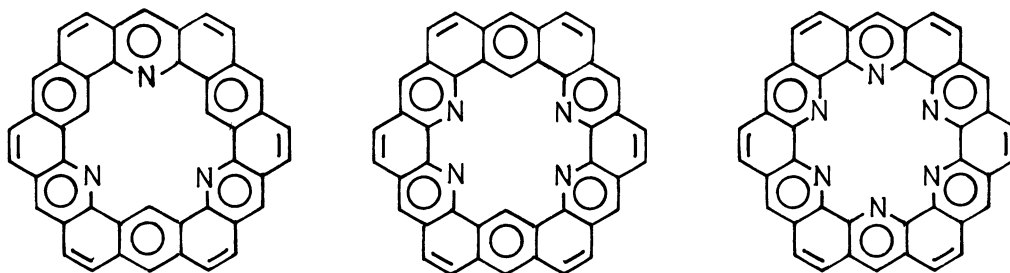


Fig. 7. A triaza-kekulene, a tetraaza-kekulene, and the hexaaza-kekulene.

A major difference between the porphyrinic and polyaza-kekulene ligands consists in the presence of two ionizable protons in the former, leading to different valence states of coordinated metals. To make the polyaza-kekulene ligand more similar to porphyrins, one can :

(i) convert all, or some of, the pyridine nuclei into 4H-pyridone rings (if only part of the pyridine rings become pyridones, the symmetry in the ligand

is lost), or

(ii) substitute other hydrogen atoms by $-(\text{CH}_2)_m-\text{CO}_2^-$ or by $-(\text{CH}_2)_m-\text{SO}_3^-$ groups where $m = 0, 1, 2$, etc., ensuring thereby electrical neutrality of the complex with metallic cations M^{n+} . In the absence of any of these two alternatives, the polyaza-kekulene ligands resemble from the electrical standpoint the crown ethers or cryptands.

In our laboratory, Extended Hückel calculations (in collaboration with Dr. M. Elian from Bucharest, and Dr. G. Surpățeanu from Jassy, Roumania) have been delayed owing to the small capacity of our computers, but it is hoped that these difficulties will be circumvented in the future.

So far, no polyaza-kekulene has been prepared ; this is an exciting synthetic challenge for organic chemists.

"LOCAL RING CURRENTS" OR "BENZENE CHARACTERS" IN CATAFUSENE SYSTEMS

On the basis of electronic absorption spectra, Clar postulated (Ref. 38) that aromatic sextets are localized in certain rings of polycyclic benzenoid systems, and he devised certain rules for knowing when to write circles in these rings, and when to write double bonds. These qualitative ideas gained a quantitative support by means of theoretical calculations initiated by Polansky and Derflinger (Ref. 39), and continued by Dewar, Herndon, Randić, Kruszewski, Hosoya, Aihara, Gutman, and Bonchev with their co-workers (Refs. 40-49). Table 5 collects illustrative data for anthracene, showing clearly that, in agreement with Clar's ideas, the marginal rings have a larger resonance energy than the central ring (only Herndon's and some of Randić's data lead to the opposite result). If, as will be defined further in more detail, f is the relative resonance energy of a ring in a PAH versus the benzene resonance energy and if f_3 and f'_3 refer to the marginal and central rings in anthracene, respectively, then the data from Table 5 indicate that $f_3 > f'_3$.

TABLE 5. Comparison of relative resonance energies for individual rings in anthracene after various authors.

A u t h o r s	Ref.	Marginal ring	Central ring
Polansky & Derflinger	39	0.893 B	0.840 B
Dewar & De Llano	40	0.277 eV	-0.139 eV
Herndon & Ellzey	42	0.600	0.700
Randić	43	0.3655	0.3612
Randić	44	0.500	0.500
Aihara	45	0.151 B	0.120 B
Gutman & Bosanac	46	0.0951 B	0.0652 B
Aida & Hosoya	47	0.678 B	0.518 B
Randić	48	0.521 eV	0.558 eV

So far, no experimental checking of these ideas has been attempted using ^1H -NMR spectra. We have tried to solve this problem by means of proton NMR spectra of N-aryl-2,4,6-trimethylpyridinium salts. Such salts are readily available from primary arylamines and 2,4,6-trimethylpyrylium perchlorate (which is easily prepared, Ref. 50, from simple starting materials : t-butanol, acetic anhydride, and perchloric acid) or sulfoacetate (this salt is not explosive and results by replacing perchloric acid by sulphuric acid, Ref. 51). As indicated earlier (Refs. 1, 52), the ring current in the N-aryl group shields the six α -standing methyl protons and deshields the three γ -standing methyl protons. The difference in chemical shift is a measure of the ring current in the N-aryl group. We proposed the expressions

$$D = \delta(\gamma\text{-Me}) - \delta(\alpha\text{-Me}_2) \quad \text{and} \quad \text{RRC} = 200(D + 0.25)$$

for the relative ring current (RRC) having N-phenyl-2,4,6-trimethylpyridinium perchlorate in trifluoroacetic acid as standard with RRC = 100. The expression

for RRC is valid for five- and six-membered aromatic or heterocyclic groups having no ortho-substituents. When ortho-substituents are present, RRC is higher in some cases (but there is no regular trend), probably owing to variations in the time-averaged dihedral angle between the pyridinium and N-aryl rings (Ref. 53).

A more detailed insight on the shielding and deshielding effects is provided by the differences between corresponding proton chemical shifts of N-aryl and N-methyl derivatives of these 2,4,6-trimethylpyridinium salts. Since the difference of chemical shifts between α and γ methyl protons in 1,2,4,6-tetramethylpyridinium perchlorate is $2.82 - 2.58 = 0.24$ ppm, it is evident that the difference D' between the relative (de)shieldings when both are calculated with 1,2,4,6-tetramethylpyridinium as standard will be $D' = D + 0.24$.

Table 6 presents the experimental results when the N-aryl group is phenyl, naphthyl or anthryl in N-aryl-2,4,6-trimethylpyridinium salts obtained from 2,4,6-trimethylpyridinium perchlorate and all possible monoarylamines derived from benzene, naphthalene and anthracene (Ref. 53).

TABLE 6. Experimental and calculated $^1\text{H-NMR}$ (de)shielding of α (γ)-methyl protons in N-acenyl-2,4,6-trimethylpyridinium perchlorates relatively to 1,2,4,6-tetramethylpyridinium perchlorate (solutions in trifluoroacetic acid at room temperature, all values in ppm).

N-Aryl substituent	Experimental determinations					Calculated values					
	Chemical shifts, δ		Relative (de)shieldings			Data from Ref. 54 Johnson-Bovey			Data from Ref. 55 Haigh-Mallion		
	α -Me	γ -Me	α -Me	γ -Me	D'	α -Me	γ -Me	D'	α -Me	γ -Me*	D'
Ph	2.48	2.73	0.34	-0.15	0.49	0.37	-0.09	0.46	0.15	-0.03	0.18
2-Naph	2.54	2.78	0.28	-0.20	0.48	0.35	-0.11	0.46	0.14	-0.03	0.17
2-Anth	2.55	2.73	0.27	-0.15	0.42	0.35	-0.11	0.46	0.13	-0.03	0.16
1-Naph	2.43	2.86	0.39	-0.28	0.67	0.45	-0.15	0.60	0.18	-0.04	0.22
1-Anth	2.40	2.80	0.42	-0.22	0.64	0.41	-0.19	0.60	0.17	-0.04	0.21
9-Anth	2.29	2.97	0.53	-0.39	0.92	0.53	-0.21	0.74	0.21	-0.05	0.26
Me	2.82	2.58	0.00	0.00	0.00	-	-	-	-	-	-

* Approximate values.

Assuming for the moment equal ring currents in all rings of the N-acenyl group and assuming that these ring currents are the same as in an N-phenyl group, we calculated (de)shielding effects for α - and γ -methyl protons at various dihedral angles θ between the pyridinium and aryl rings, using both the data of Johnson and Bovey (Ref. 54), and the newer revised data of Haigh and Mallion (Ref. 55). Table 6 presents the results for $\theta = 90^\circ$, considering the C-N⁺ inter-ring bond distance as being approximately equal to the benzene C-C bond distance. This latter bond distance is the unit for the z and ρ parameters used in these calculations (Refs. 54,55). Since the methyl groups are supposed to be freely rotating, the position of the protons is taken at the intersection of the plane determined by the three methyl protons with the line continuing the C(ring)-C(methyl) bond, as seen in Fig. 8.

It will be observed that α -methyl protons may be shielded or deshielded by the N-aryl ring, whereas the γ -methyl group, which is always in the plane of the N-aryl ring, will be always deshielded. These (de)shielding values were determined from z and ρ parameters measured with Dreiding models. Fig. 8 presents the principle defining the z and ρ parameters. In Table 7 we exemplify these calculations using the Johnson-Bovey data; in these cases, the (de)shielding values were determined graphically, therefore the precision is low. However, for distances between the benzene ring and the (de)shielded proton(s) which are not too large (in our case this means for effects on α -methyl protons), the Haigh-Mallion data, in tabular form, are much more accurate; in the case of γ -methyl protons, on the other hand, the distances are so large that the Haigh-Mallion tables must be converted into graphical form and extrapolated leading to less precise values in Table 6, as indicated by the appended footnote to that Table.

TABLE 7. Data for (de)shielding, in ppm, caused by individual benzenoid rings of N-aryl-2,4,6-trimethylpyridinium salts after Johnson and Bovey, assuming orthogonal rings ($\theta = 90^\circ$)

N-Aryl ring	Parameters*		(De)shielding (in ppm)	
	z	ρ	α -Me	γ -Me
Phenyl	2.2	1.8	0.37	-0.09
Additional ring of 2-naphthyl	2.2	3.4	-0.02	-0.02
Additional ring of 2-anthryl	2.2	5.1	-0.01	-0.01
Additional ring of 1-naphthyl	2.2	2.5	0.08	-0.06
Additional ring of 1-anthryl**	2.2	3.8	-0.04	-0.04

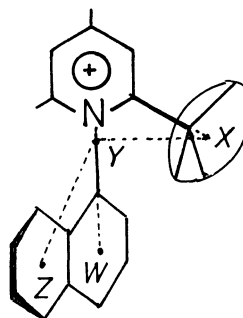
* In units equal to the C-C bond distance of benzene.

**The additional ring is relative to the N-phenyl, excepting for the 1-anthryl group which is considered in addition to naphthalene. The 9-anthryl group is calculated as having two additional rings of 1-naphthyl groups.

For the α -methyl protons, assuming orthogonal pyridinium and N-aryl rings, the parameters z and ρ are defined as follows :

Shielding by the N-phenyl ring,
z = XY ; ρ = YW

Shielding by the additional
1-naphthyl ring,
z = XY ; ρ = YZ



All lengths in units equal to the benzene C-C bond length.

Fig. 8. Definitions of (de)shielding parameters for N-aryl-2,4,6-trimethylpyridinium salts. It may be seen that for a γ -methyl group, z = 0 irrespective of the dihedral angle θ .

We will now show how one can calculate, in principle, "local ring currents" or "benzene characters" of PAH's from our NMR data. Let the local ring currents in successive rings, starting from the margin of a non-branched symmetrical catafusene, e. g. an acene with n rings, be denoted by f_n, f'_n, f''_n , etc. (relative to the ring current of benzene). Then, if the (de)shielding due to the global ring current is g_n , we have (based on the Johnson-Bovey data from Table 6) :

System	N-Aryl	Shielding of α - (2 and 6-)methyl protons
1	Phenyl	$0.34 = 0.37 f_1$
2	2-Naphthyl	$0.28 = 0.37 f_2 - 0.02 f'_2 + g_2$
	1-Naphthyl	$0.53 = 0.37 f_2 + 0.08 f'_2 + g'_2$
3	2-Anthryl	$0.27 = 0.37 f_3 - 0.02 f'_3 - 0.01 f''_3 + g_3$
	1-Anthryl	$0.39 = 0.37 f_3 + 0.09 f'_3 - 0.04 f''_3 + g'_3$
	9-Anthryl	$0.42 = 0.37 f_3 + 0.08 f'_3 + 0.08 f''_3 + g''_3$

Similar systems of equations could be written also for the deshielding of γ - (4-)methyl protons. In the above equations, g_2 and g'_2 are related to one another by geometrical data referring to the relative positions of the centres of naphthyl circuits, and similarly g_3, g'_3 and g''_3 only constitute one unknown because one can calculate geometrically the relative positions of the centres of anthryl circuits substituted in 1, 2, or 9, with respect to the α -methyl group. We thus obtain system 1 of one equation with one unknown (the actual value of f_1 should be found equal to 1.00, but the difference is small), system 2 of two equations with two unknowns (f_2 and the global ring current g_2, g'_2 the two latter parameters being interrelated geometrically), and system 3 of three equations with three unknowns (f_3, f'_3 and the global ring current in

anthracene, by interrelating geometrically g_1 , g_2 and g_3 according to the substitution patterns, 2 (β), 1 (α) and 9 (meso), respectively. Such calculations are in progress and will be reported later.

From X-ray diffraction of single crystals of N-phenyl-2,4,6-trimethylpyridinium perchlorate (Ref. 56), it is known that in the crystal the dihedral angle is 85° and that the C-N⁺ bond distance is 1.46 Å. However, in solution, the dihedral angle (and probably also the C-N⁺ bond distance) may differ, as indicated by the effect on D and D' of certain ortho-substituents such as methyl (Refs. 52, 53). An indication that the C-N⁺ bonds are appreciably shorter than C-C bonds is provided by the higher rotation barriers exhibited by N-isopropylpyridinium salts relative to C-isopropylpyridines or C-isopropylpyridinium salts (Ref. 57).

If the calculated data had been larger than the experimental ones, then one could have computed local ring currents in the anthryl group neglecting (in the first approximation) the global ring current. However, the highest calculated (de)shielding effects (namely assuming orthogonal rings and local ring currents equal to those of benzene in Tables 6 and 7, but not in the systems 1-3 of equations) are lower than, or equal to, the experimentally determined values, as shown by Table 6. The more accurate Haigh-Mallion data lead to much lower calculated values than the experimental values. Therefore one has to assume that in addition to local ring currents the (de)shielding is also due to a ring current over the whole acenyl group; this global ring current seems to be much higher (at least with the Haigh-Mallion data) than the local ring currents. Owing to the other unknown parameters (dihedral angle and the C-N⁺ bond angle, two connected data which are known in the crystal but not in solution), the computation of local ring currents in the N-anthryl group is bound to be rather approximate. For a more precise calculation of such local ring currents, the calculated (de)shieldings exerted by a phenyl group should be known with a higher accuracy and over a wider range of interatomic distances than that afforded by the Johnson-Bovey or even the Haigh-Mallion data.

Of course, in the context of the present symposium, one must bear in mind that ring currents, conjugation energies, and aromaticity, are correlated notions but their magnitudes need not be proportional (Ref. 58).

To conclude this Section, I would like to mention interesting observations concerning the Aromatic Solvent Induced Shifts (ASIS) in the proton NMR spectra of N-anthryl-2,4,6-trimethylpyridinium perchlorates. To weighed amounts of the three isomeric perchlorates mentioned above (in trifluoroacetic acid at room temperature, in 5 mm outer diameter NMR vials), progressively larger amounts of hexadeuterobenzene were added. A remarkable behaviour was noted for the chemical shifts of α - and γ -methyl protons: for the 2-anthryl-, 1-anthryl-, and 9-anthryl-group, respectively, the ASIS values are the following, on increasing the hexadeuterobenzene concentration till the asymptotic limit is reached in a solvent mixture containing the minimal amount of trifluoroacetic acid to keep the salt in solution; in all cases the aromatic solvent causes upfield shifts. All data in Table 8 are expressed in Hz, and the NMR instrument was an A-60A Varian instrument.

TABLE 8. ASIS Data for N-anthryl-2,4,6-trimethylpyridinium perchlorate in trifluoroacetic acid - hexadeuterobenzene on increasing from zero to the limiting value the concentration of hexadeuterobenzene (all data in Hz with a 60 MHz instrument)

N-Aryl	Chemical shift difference (γ - α)			Upfield chemical shifts	
	From	To	Diff.	γ -Me	α -Me
2-Anth	12	21.5	9.5	28.5	40.5
1-Anth	24	35.0	11.0	30.5	42.0
9-Anth	41	53.5	12.5	30.0	45.0

It is apparent from Table 8 that the ASIS (Ref. 59) operates more strongly in the 9-anthryl derivative (the ¹H-NMR shielding of α -methyl groups due to the deuterobenzene molecules crowding around the 9-anthryl group which is closest to the α -methyl groups is therefore the strongest), and less strongly in the 2-anthryl derivative, with the anthryl group pointing away from the α -methyl groups. The 1-anthryl derivative occupies an intermediate position for ASIS effects. The three N-anthryl derivatives are illustrated in Fig. 9.

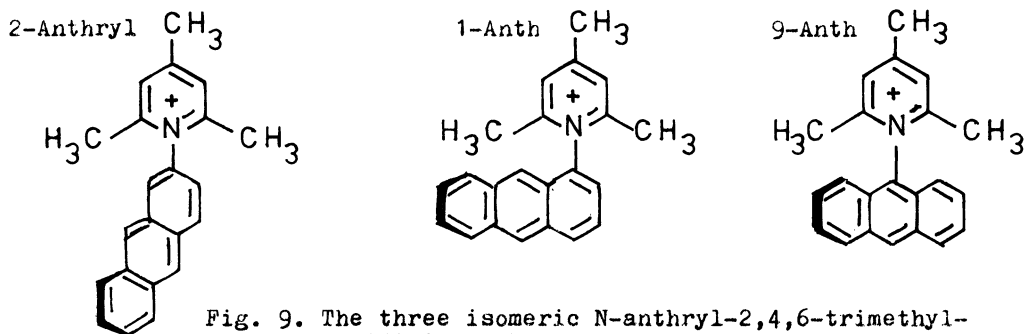


Fig. 9. The three isomeric N-anthryl-2,4,6-trimethylpyridinium salts.

TWO CLASSES OF DIRADICALS WITH POLYHEX SKELETONS

In the following discussion, unless otherwise stated, we shall deal only with peri-condensed polyhexes (PAH's) having no side-chains. According to the Coulson-Rushbrooke starring procedure, all carbon atoms of these alternant PAH (bipartite graphs) belong either to the starred, more numerous, set, or to the unstarred set, so that no atom (vertex) of one set is adjacent to an atom of the same set (Refs. 19, 60). All systems to be discussed in this Section will be supposed to be exclusively composed of sp^2 -hybridized carbon atoms, so that π -electrons will not be explicitly shown. Some caution is necessary, because some of the following graphs will be constitutional hydrogen-depleted graphs with vertices symbolizing carbon atoms and edges symbolizing covalent bonds, while other graphs will be dualist graphs with other meanings of vertices and edges.

It is easy to recognize free radicals such as monoradicals, triradicals, and in general $(2k+1)$ -radicals. All these odd-alternant systems have an odd number of carbons, and hence the number of starred atoms is higher than that on non-starred atoms. The number s of spins equals the difference between the cardinals of the two sets of atoms, as seen in Fig. 10.

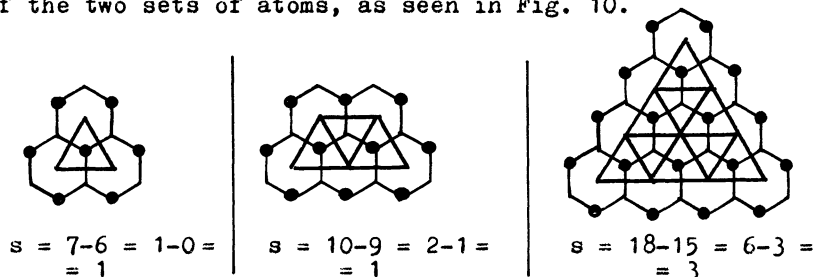


Fig. 10. Monoradicals or polyradicals (s -radicals) with odd $s = 2k + 1$.

The even-alternant systems, on the other hand, may be normal systems (possessing at least one Kekulé structure) or $2k$ -radicals (diradicals, tetraradicals, etc.). If the two sets of starred and non-starred atoms have different cardinals, their difference again equals the number s of spins, as seen in Fig. 11.

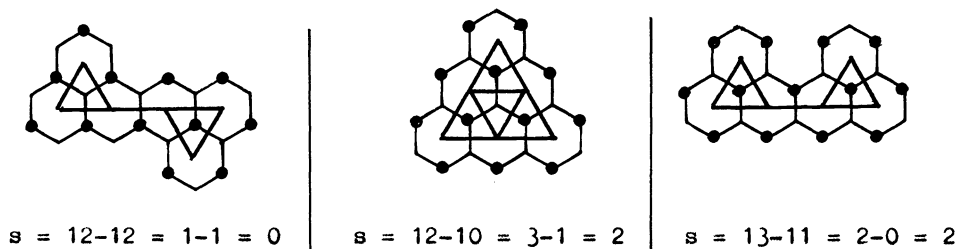


Fig. 11. Normal compounds ($s = 0$) or diradicals with even $s = 2k$.

We call this type of diradicals D-diradicals because the two cardinals are Different. It is easy to demonstrate that such D-diradicals cannot have a Kekulé structure, or in graph-theoretical terms that such graphs do not have a decomposition into 1-factors, or a dimer covering: imagine that a π -bond

(corresponding to a 1-factor, or a dimer, i. e. a simple graph consisting of two vertices joined by one edge) has differently coloured endpoints ; if these are the colours of the two sets, it results that no Kekulé structure is possible in this case.

If, on the other hand, the numbers of starred and non-starred atoms are equal, the compound may be normal or may be a $2k$ -radical. We call such diradicals S-diradicals because they have the Same cardinals of the two sets. Examples of such S-diradicals will be presented and discussed in this Section at length for structures derived from polyhexes. Here we wish to mention that normal (closed-shell) compounds, and polyradicals or open-shell structures (both D-monoradicals or D-diradicals, and S-diradicals) also exist in the case of acyclic compounds or cyclic compounds with side-chains, as seen in Fig. 12.

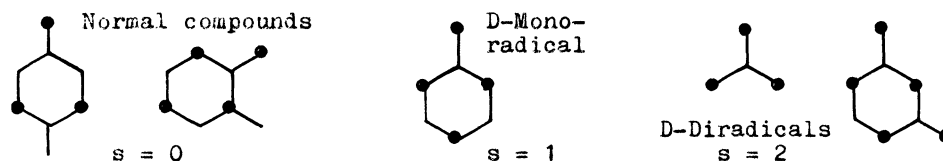


Fig. 12. Examples of normal compounds or polyradicals with side-chains.

Returning to structures based on polyhexes, we shall present in the following a simple method for determining :

- (i) the number of spins in $(2k+1)$ -polyradicals or D- $2k$ -radicals with PAH structures ;
- (ii) the difference between the cardinals of the two sets for any PAH, on the basis of the dualist graph, without counting the carbon atoms (Ref. 61) ; and
- (iii) the difference between a normal, closed-shell PAH with at least one Kekulé structure, and an S- $2k$ -polyradical, although both these polyhexes have the same $s = 0$ difference between the two cardinals (therefore this difference s , defined on the basis of the cardinals of the starred and non-starred sets, is not always equal to the number of spins).

Examination of the first and third isomeric structures from Fig. 11, which represent a normal closed-shell compound (zethrene) and a D-diradical, respectively, shows an interesting difference, which may be generalized : in the D-diradical, both vertices of the constitutional graph which are situated at the centres of the three-membered rings of the dualist graphs belong to the same set (starred vertices, depicted as black dots), while in the closed-shell (normal) compound they belong to different sets (one starred, one non-starred vertex). We must draw the attention of the reader that unlike previous Sections, here the heavy dots will no longer symbolize vertices of the dualist graphs, but atoms belonging to the starred set.

The dualist graph of a plane "honeycomb" graphite lattice (of which any polyhex is a subgraph) is a triangulated plane. Fig. 13 presents a portion of this plane with the two graphs. Note that we adopt the convention that we draw the benzenoid rings so that some C-C bonds appear vertically, and no C-C bond is horizontal. In this case, the dualist graph (triangulated plane) necessarily has horizontal lines. Considering only the triangulated plane, it may be seen that six triangles meet at each point, three of which have a starred centre and the remaining three an unstarred centre. The situation is represented more clearly by the second drawing in Fig. 13 which no longer shows the honeycomb lattice corresponding to the constitutional graph, but only the triangulated plane, i. e. the dualist graph ; in this drawing, the starred- and non-starred-centre triangles are drawn in black and white, respectively, as if the star had filled the whole triangle. The result is a triangulated chessboard.

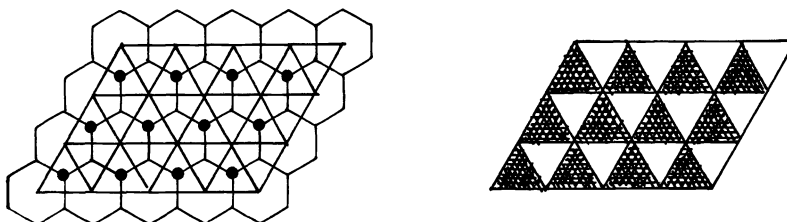


Fig. 13. The starred honeycomb lattice and its dualist graph

An essential observation is that for the adopted orientation wherein all triangles have a horizontal side, the black triangles always point upwards, and the white triangles always point downwards. Thus there exist only two species of triangles (starred or non-starred in their centres which is time-consuming to establish, or black and white, i. e. upward or downward pointing, which is visible at a glance).

If one colours accordingly the properly-oriented triangles of the dualist graph of any perihex it is easy to calculate s as the difference between the number of black (or centre-starred) and the number of white (centre-non-starred) triangles. Figures 11 and 12 prove that s is the same as from the the classical Coulson-Rushbrooke starring approach. It is also seen, however, that the present procedure is much simpler because the dualist graph has a much lower number of triangles than the vertices of the constitutional graph, so that in the present procedure s results as the difference between two small numbers which may be determined by visual inspection while in the classical procedure s resulted as the difference between two large numbers which had to be determined with pencil and paper so that mistakes could occur more frequently for large structures.

Returning now to the last problem (iii) mentioned in the introduction to this Section, namely to discriminate between normal (closed-shell) structures, D-diradicals, and S-diradicals (or -polyradicals with even numbers of spins), the procedure just mentioned distinguishes easily between D- $2k$ -radicals with non-zero s values ($s = 2k$), on one hand, and between systems with $s = 0$ which may be either normal systems or S- $2k$ -radicals. Fig. 14 presents examples of all three types of structures. For simplicity, only the dualist graphs are shown, and since the numbers of triangles is quite small, they are not coloured in black and white (this may be done mentally looking at the upward- and downward-pointing triangles, respectively).

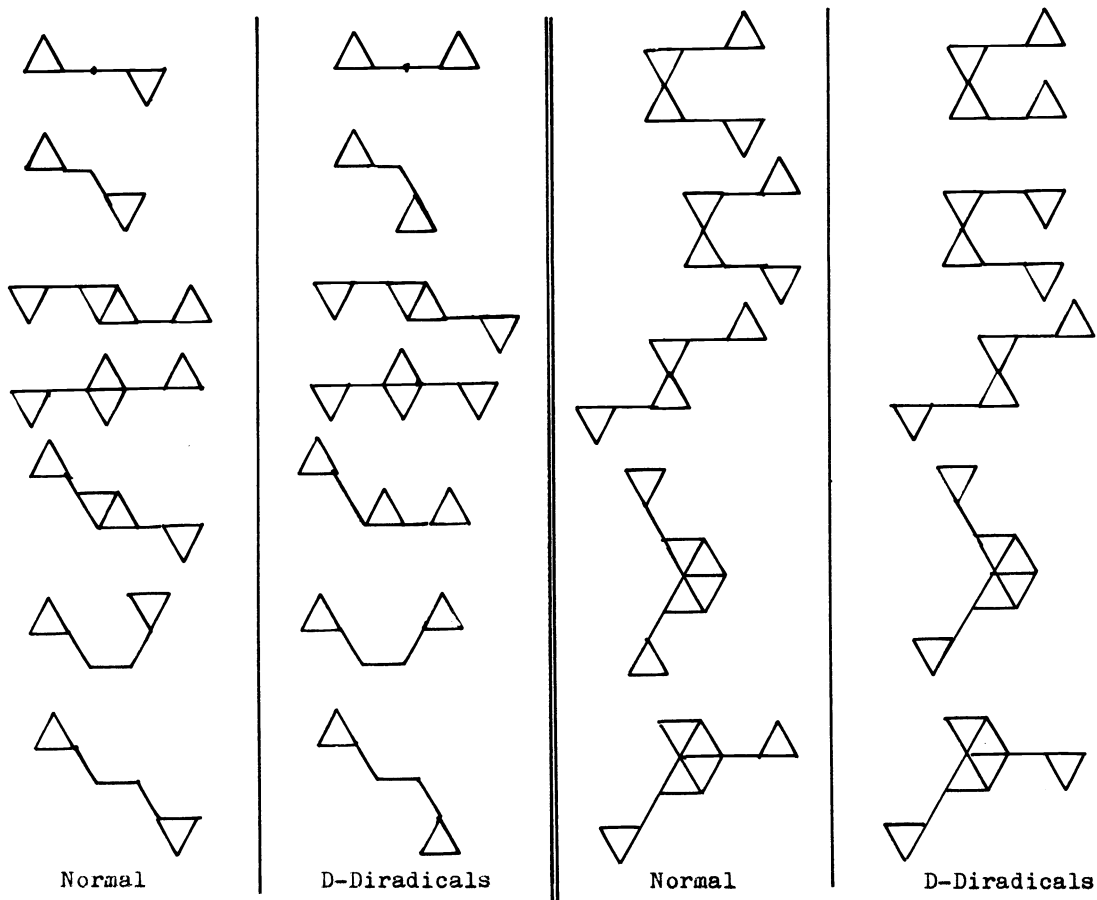


Fig. 14. Further examples (see also Fig. 11) of normal and D-diradicalic PAH structures (presented here as their dualist graphs), continuing on next page with normal, D-, and S-diradicals

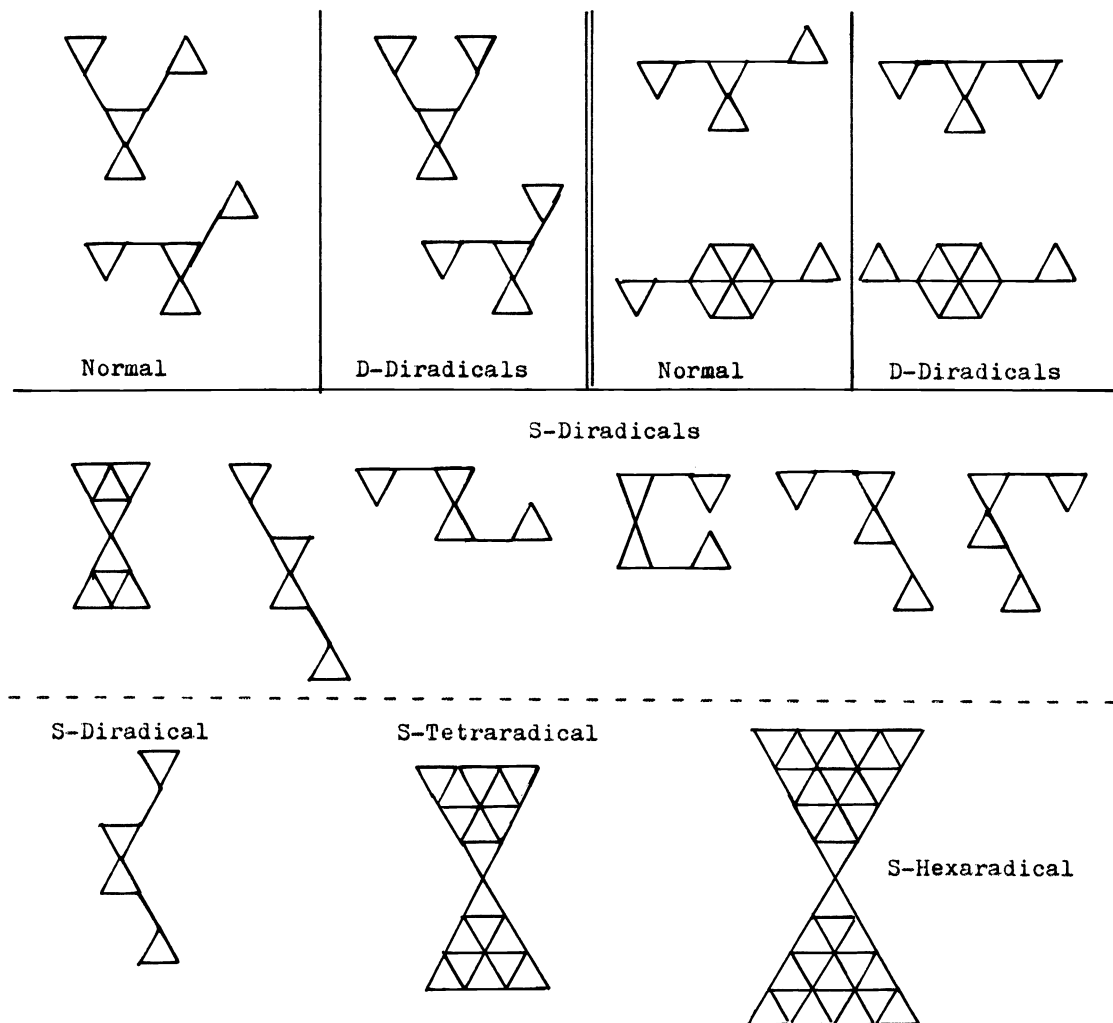


Fig. 14 (continued). Examples of normal polyhexes with $s = 0$, of D-diradicals with $s = 2$, and of S- $2k$ -radicals with $s = 0$.

Independently, Gutman (Ref. 62) and Mallion (Ref. 63) observed that there exist both normal (closed-shell) PAH structures and open-shell (triplet) diradicals having equal numbers of starred and non-starred carbon atoms, i. e. $s = 0$. Gutman and Mallion both found the first S-diradical from Fig. 14, and Gutman also found the second S-diradical from the same figure. The remaining S-polyradicals from Fig. 14 are displayed for the first time. This means that $s = 0$ is a necessary but insufficient condition for a PAH to be normal one: it can also be a $2k$ -radical for which no Kekulé structure can be written. All such $2k$ -radicals (belonging to the class we call S- $2k$ -radicals) so far known have a central perylene structure, as evident from Fig. 14.

A general rule allowing to discriminate polyhex S-diradicals from normal compounds is the following:

dualist graphs of S-diradicals are formed from two dualist graphs of D-diradicals by "fusion" of a vertex; since this common vertex is an apex of a triangle, this means that the two D-diradicals share a common benzenoid ring, and this explains why a central perylene system occurs in all S-diradicals.

This rule can be easily generalized to S- $2k$ -radicals formed from two D- $2k$ -radicals sharing a vertex at the apex of a triangle. Of course, to yield an S-diradical when two D-diradicals become thus fused, the orientations of triangles in dualist graphs are opposite so that the numbers of black and white triangles become equal, hence $s = 0$. It is easy to see that by breaking the S- $2k$ -radicals from Fig. 14 into two fragments at the central junction of the perylene moiety, two D- $2k$ -radicals result in all cases.

This rule allows the construction of numerous, actually of an unlimited number of S-2k-radicals, as indicated in Fig. 15. The same Fig. 15 also shows that this rule is not limited to S-2k-radicals with polyhex structure : by fusion (sharing) of a C-C bond, two acyclic D-diradicals like trimethylene-methane form analogously acyclic S-diradicals (for clarity, in this case the starred atoms are shown by black dots) ; the resulted tetramethylene-ethene has equal numbers of starred and non-starred atoms, and is therefore an acyclic S-diradical. Indeed, this structure is included among other diradicals in a paper by Herndon and Ellzey Jr. (Ref. 64). Both D-diradicals and S-diradicals share the properties that they possess two singly-occupied non-bonding levels and that their formulas do not admit decompositions into 1-factors, or what is the same thing, they have no Kekulé structures.

According to the procedure described by Herndon (Ref. 65), it is easy to recognize the presence of non-bonding levels in all these structures, excizing chains and/or rings of known closed-shell stable structures from the periphery towards the centre. Fig. 16 shows excisions of naphthalene structures by indicating the sectioned C-C bonds in dashed lines. The remaining dimethyleneperylenes are evidently diradicals. Similarly, excizing from the first S-diradical from Fig. 14 two anthracene structures (the top and bottom rows of benzenoid rings), one obtains 1,2,4,5-tetramethylenebenzene which is a diradical. On excizing from the S-tetradiradical in Fig. 14 similarly two tetracene structures, one obtains a tetramethylene-perylene, i. e. a tetradiradical, etc.

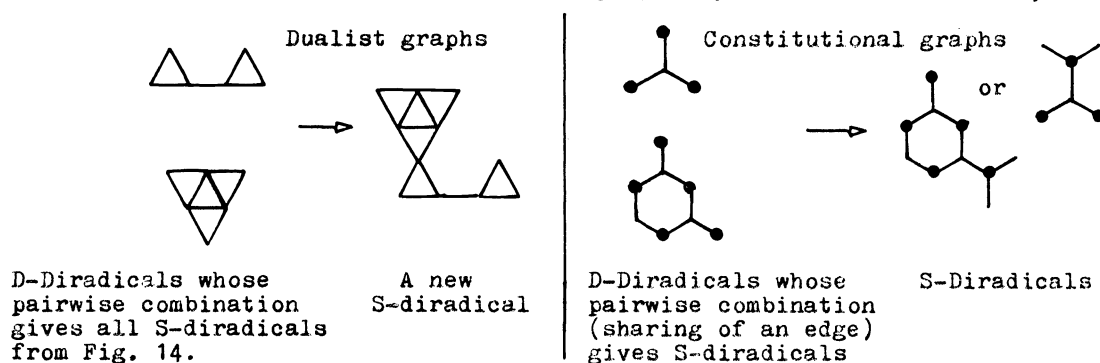


Fig. 15. Construction of S-diradicals from two D-diradicals : if the D-diradicals are polyhexes, they share a benzenoid ring ; if they are acyclic, they share a C-C bond.

By means of graph-theoretical matrices it is also possible to determine whether a given graph has, or does not have, a Kekulé structure (a decomposition into 1-factors, or a dimer covering). For PAH's the Kekulé structure count SC and the corrected structure count are identical and they are given by

$$SC = |\det \underline{A}|^{1/2} = \det \underline{B}$$

where \underline{A} is the symmetrical adjacency matrix, and \underline{B} is the non-symmetrical matrix in the form expressed by Ham (Ref.66), having vertices of the starred set as row headings, and vertices of the non-starred set as column headings ; entries in both matrices a 1 for adjacent vertices and 0 for non-adjacent vertices. Since for (2k+1)-radicals and for D-2k-radicals the numbers of rows and columns are different in the B-matrices, the corresponding determinants have value zero. For discriminating between normal structures and S-2k-radicals, one has to solve the determinants of the A- or B-matrices, a much more tedious procedure than that described here.

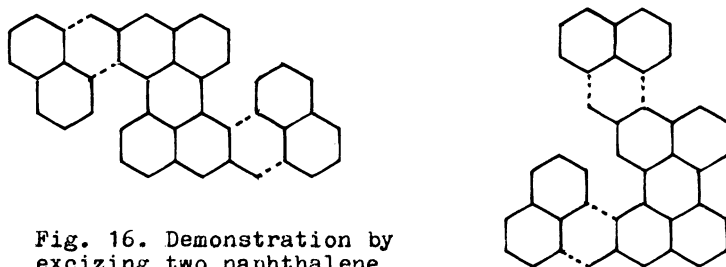


Fig. 16. Demonstration by excizing two naphthalene subgraphs from S-diradicals (whose dualist graphs are the third and sixth in Fig. 14) that these structures have two unpaired spins (dimethyleneperylenes are left).

Acknowledgements - Thanks are expressed to : Professor W. Schmidt for providing data prior to publication and for permission to use them in correlations ; to Drs. R. B. Mallion, N. Trinajstić and I. Gutman for discussions ; to Professors J. J. Kaufman and W. S. Koski for their initiative to develop the computer program, and to Dr. K. Balasubramanian for implementing it ; and to Dr. M. Elian, O. Dragomir-Filimonescu, I. Moțoc, J. Vosganian for help in computations ; last, but not least, to Dr. A. Dinulescu, Dr. F. Chiraleu, F. Iordache and D. Pătrășcoiu for experiments with N-aryl-trimethylpyridinium salts. The most cordial thanks are addressed to Prof. I. Agranat for his kindness.

REFERENCES

1. A. T. Balaban, Pure Appl. Chem. **52**, 1409 (1980).
2. A. T. Balaban and F. Harary, Tetrahedron, **24**, 2505 (1968).
3. A. T. Balaban, Tetrahedron, **25**, 2949 (1969).
4. D. Bonchev and A. T. Balaban, J. Chem. Inf. Comput. Sci. (in press).
5. I. Agranat, B. A. Hess and L. J. Schaad, Pure Appl. Chem. **52**, 1399 (1980).
6. F. Harary and R. C. Read, Proc. Edinburgh Math. Soc. **17**, 1 (1970).
7. O. E. Polansky and D. H. Rouvray, Math. Chem. **2**, 63, 91 (1976).
8. O. E. Polansky and D. H. Rouvray, Math. Chem. **3**, 97 (1978).
9. A. T. Balaban, Rev. Roumaine Chim. **21**, 1049 (1976) ; Math. Chem. **2**, 51 (1976).
10. A. T. Balaban and P. v. R. Schleyer, Tetrahedron, **34**, 3599 (1978).
11. A. T. Balaban, Rev. Roumaine Chim. **15**, 1243 (1970).
12. A. T. Balaban, Rev. Roumaine Chim. **22**, 45 (1977).
13. H. Hosoya and T. Yamaguchi, Tetrahedron Letters, 4659 (1975).
14. A. T. Balaban, A. Chiriac, I. Motoc and Z. Simon, Steric Fit in Quantitative Structure-Activity Relations, Lecture Notes in Chemistry No. 15, p. 22, Springer, Berlin (1980).
15. D. Biermann and W. Schmidt, J. Am. Chem. Soc. **102**, 3163, 3173 (1980).
16. D. H. Rouvray, in Chemical Applications of Graph Theory (ed. A. T. Balaban), p. 175, Academic Press, London (1976).
17. A. Graovac, I. Gutman and N. Trinajstić, Topological Approach to the Chemistry of Conjugated Molecules, Lecture Notes in Chemistry No. 4, Springer, Berlin (1977).
18. I. Gutman and N. Trinajstić, Topics Curr. Chem. **42**, 49 (1973).
19. C. A. Coulson, B. O'Leary and R. B. Mallion, Hückel Theory for Organic Chemists, p. 149, Academic Press, London (1978).
20. T. D. Sterling and S. V. Pollack, Am. J. Public Health, **62**, 152 (1972).
21. W.-S. Tsang and G. W. Griffin, Metabolic Activation of Polynuclear Aromatic Hydrocarbons, Pergamon Press, Oxford (1979).
22. A. Pullman and B. Pullman, Adv. Cancer Res. **3**, 117 (1955) ; Idem, in Jerusalem Symp. on Quantum Chem. and Biochem. I. Physico-Chemical Mechanisms of Carcinogenesis (eds. E. D. Bergmann and B. Pullman), p. 9, The Israel Acad. Sci. and Humanities, Jerusalem (1969) ; I. Berenblum, ibid. p. 321.
23. P. Daudel and R. Daudel, Biol. Med. **39**, 201 (1950).
24. D. M. Jerina et al., in In Vitro Metabolic Activation in Mutagenesis Testing (eds. F. J. de Serres et al.), p. 159, Elsevier, Amsterdam (1976).
25. D. M. Jerina and J. W. Daly, in Drug Metabolism (eds. D. V. Parke and R. L. Smith), p. 13, Taylor and Francis Ltd., London (1976).
26. D. M. Jerina et al., in Drug Design and Adverse Reactions (eds. H. Bundgaard et al.), Alfred Benzon Symp. X, p. 261, Munksgaard, Copenhagen, Denmark (1977).
27. K. Balasubramanian, J. J. Kaufman, W. S. Koski and A. T. Balaban, J. Comput. Chem. **1**, 149 (1980).
28. A. Dipple, in Chemical Carcinogens (ed. C. E. Searle), ACS Monograph 173, p. 245, Am. Chem. Soc., Washington, D. C. (1976).
29. J. Iball, Am. J. Cancer, **35**, 188 (1939).
30. J. C. Arcos, M. F. Argus and G. Wolf, Chemical Induction of Cancer, vol. 1, p. 414, Academic Press, New York (1968).
31. W. C. Herndon, Trans. N. Y. Acad. Sci., Ser. II, **36**, 200 (1974) ; Quantum Biology Symp. No. 1, 123 (1974).
32. G. D. Berger, I. A. Smith, P. G. Seybold and M. P. Serve, Tetrahedron Letters, 231 (1978).
33. F. Diederich and H. A. Staab, Angew. Chem. **90**, 383 (1978).
34. C. Krieger, F. Diederich, D. Schneizer and H. A. Staab, Angew. Chem. **91**, 733 (1979).
35. R. Mc Weeny, Proc. Roy. Soc. A **64**, 261, 921 (1951) ; G. Ege and H. Fischer, Tetrahedron, **23**, 149 (1967).
36. H. A. Staab and F. Binnig, Chem. Ber. **100**, 293 (1967).

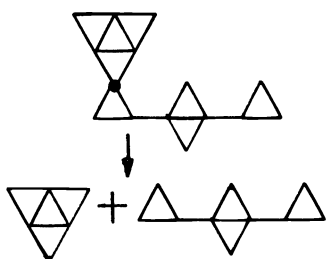
37. W. Jenny and R. Peter, Angew. Chem. **77**, 1027 (1965) ; Angew. Chem. Int. Ed Engl. **4**, 979 (1965).
38. E. Clar, The Aromatic Sextet, Wiley, London (1972) and further references therein ; Chimia, **18**, 375 (1964) ; E. Clar and I. A. Macpherson, Tetrahedron, **18**, 1411 (1962) ; E. Clar and A. McCallum, ibid. **10**, 171 (1960).
39. O. E. Polansky and G. Derflinger, Int. J. Quantum Chem. **1**, 379 (1967).
40. M. J. S. Dewar and C. De Llano, J. Am. Chem. Soc. **91**, 789 (1969).
41. J. Kruszewski, Acta Chim. Lodz, **16**, 77 (1971).
42. W. C. Herndon and M. L. Ellzey, Jr., J. Am. Chem. Soc. **96**, 6631 (1974).
43. M. Randić, Tetrahedron, **30**, 2067 (1974).
44. M. Randić, Tetrahedron, **31**, 1477 (1975).
45. J. Aihara, J. Am. Chem. Soc. **99**, 2048 (1977).
46. I. Gutman and S. Bosanac, Tetrahedron, **33**, 1809 (1977).
47. M. Aida and H. Hosoya, Tetrahedron, **36**, 1317 (1980).
48. M. Randić, Pure Appl. Chem. **52**, 1587 (1980).
49. F. Pratev, D. Bonchev and V. Enchev, to appear.
50. A. T. Balaban and C. D. Nenitzescu, Org. Synth. Coll. Vol. **5**, 1106 (1973).
51. M. Dinculescu and A. T. Balaban, Org. Prep. Proc. Int. (in press).
52. A. T. Balaban, A. Dinculescu, H. N. Koutrakis and F. Chiraleu, Tetrahedron Letters, 437 (1979).
53. A. T. Balaban, A. Dinculescu, F. Iordache, F. Chiraleu and D. Pătrășcoiu, Chem. Scripta (in press).
54. C. E. Johnson and F. A. Bovey, J. Chem. Phys. **29**, 1012 (1958).
55. C. W. Haigh and R. B. Mallion, Org. Magn. Reson. **4**, 203 (1972).
56. A. Camerman, L. H. Jensen and A. T. Balaban, Acta Cryst. **25 E**, 2623 (1969).
57. C. Roussel and A. T. Balaban, to appear.
58. R. J. Abraham and W. A. Thomas, J. Chem. Soc. (B), 127 (1966) ; E. D. Bergmann and I. Agranat, in Aromaticity, Pseudo-Aromaticity, Anti-Aromaticity, The Jerusalem Symposia on Quantum Chem. and Biochem. vol. **3**, (eds. E. D. Bergmann and B. Pullman), p. 9, The Israel Acad. Sci. and Humanities, Jerusalem (1971) ; J. F. Labarre and F. Gallais, ibid. p.48
59. P. Laszlo, Progress in NMR Spectroscopy, **3**, 231 (1967) ; M. Jauquet and P. Laszlo, in Influence of Solvents on Spectroscopy (ed. M. R. J. Dack) p. 243, Wiley, New York (1975).
60. C. A. Coulson and G. S. Rushbrooke, Proc. Cambridge Philos. Soc. **36**, 193 (1940).
61. A. T. Balaban, Rev. Roumaine Chim. **26**, 407 (1981).
62. I. Gutman, Croatica Chem. Acta, **46**, 209 (1974).
63. R. B. Mallion, personal communication.
64. W. C. Herndon and M. L. Ellzey Jr., Tetrahedron Letters, 1399 (1974).
65. W. C. Herndon, J. Chem. Educ. **51**, 10 (1974).
66. N. S. Ham, J. Chem. Phys. **29**, 1229 (1958).
67. F. Harary, Graph Theory, p. 26, Addison-Wesley, Reading, Mass. (1969).
68. J. W. Essam and M. E. Fisher, Rev. Mod. Phys. **42**, 272 (1970).

APPENDIX

Procedure for distinguishing normal structures from D- or S-radicals

Definitions (Refs. 67, 68). A cut-point (cut-vertex, articulation point, separating point) of a graph is a vertex whose removal increases the number of the graph components. A cut-edge (isthmus, bridge, separating edge) of a graph is an edge (a line) whose removal also increases the number of the graph components. In particular, the deletion of a cut-point or a cut-edge of a connected graph produces a disconnected graph. In Fig. 17 the black vertex is a cut-point and the heavy line is a cut-edge.

Dualist graph with cut-point



Constitutional graphs with cut-edges

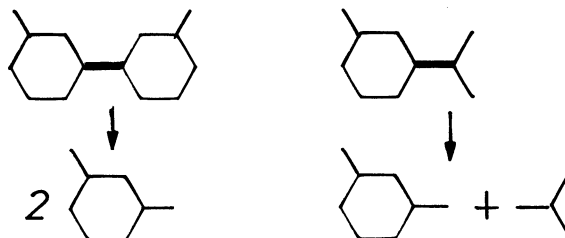


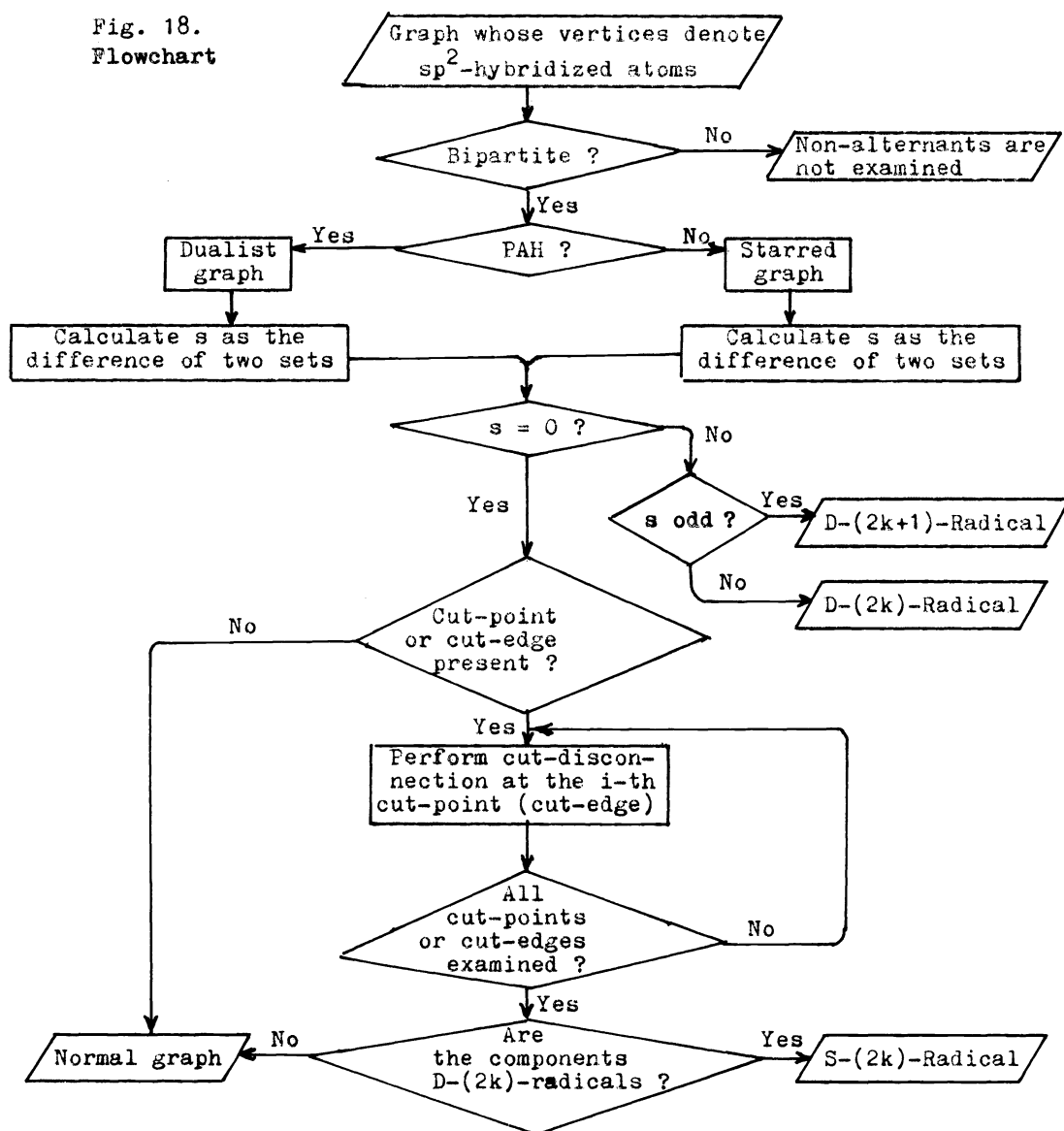
Fig. 17. Cut-disconnections of S-(2k)-radicals.

The process whereby two components of a connected graph become disjoint at a cut-point or a cut-edge, each component retaining a vertex or an edge, respectively, in the place of the original cut-point or cut-edge, respectively, will be called cut-disconnection.

A dualist graph with $2m + 1$ vertices affords on cut-disconnection two dualist graphs with $2k$ and $2(m - k + 1)$ vertices, respectively. A constitutional graph with m edges is cut-disconnected into two constitutional graphs with k , and $m - k + 1$ edges, respectively (it should be remembered that vertices of dualist graphs symbolize centres of benzenoid rings, while vertices of constitutional graphs symbolize atoms, and edges of constitutional graphs symbolize covalent bonds). Cut-disconnections are illustrated by Fig. 17.

Procedure. For skeletons of alternant, continuously-conjugated, sp^2 -hybridized compounds, the flowchart below illustrates the method for discriminating normal graphs (which have at least one Kekulé structure, i. e. one decomposition into 1-factors) from various types of radicals: odd-alternant radicals which belong always to class D, and even-alternant radicals which may belong either to the D- or to the S-classes. In the latter case, the algorithm uses the operation of cut-disconnection. To simplify the flowchart, we have not included a loop for the decision if the components after this cut-disconnection are, or are not, even-alternant D-(2k)-radicals.

Fig. 18.
Flowchart



It remains to be seen if no counter-example to this procedure will be found.